[Chem. Pharm. Bull. 33(4)1641—1651(1985)]

Prediction of Available Surface Area of Powdered Particles of Flufenamic Acid in Tablets[1)]

SHOZO KOUCHIWA,[a] MASAMI NEMOTO,[a] SHIGERU ITAI,*,[a] HIROSHI MURAYAMA[a] and TSUNEJI NAGAI[b]

Research Laboratory, Taisho Pharmaceutical Co., Ltd.,[a] Yoshino-cho-1–403, Omiya, Saitama 330, Japan and Faculty of Pharmaceutical Science, Hoshi University,[b] Ebara-2–4–41, Shinagawa-ku, Tokyo 142, Japan

(Received July 25, 1984)

A theoretical method was developed to describe the time course of the available surface area ($S(t)$) in the dissolution process of solid dosage forms. In general, dissolution of solid dosage forms includes disintegration and deaggregation (dispersion of disintegrated granules and powders), and since the mechanism is very complex, $S(t)$ in the dissolution medium cannot be determined by numerical calculation. However, the integrated value of $S(t)$, which can be considered to be the available surface area generated during the dissolution time course, can be calculated from the dissolved amount and the dissolution parameters. In addition, the ratio of the available surface area generated by time t to the total available surface generated can be regarded as a cumulative probability distribution. By the regression of this ratio ($F(t)$) to the probability distribution, the time course of $S(t)$ was able to be determined numerically. The application of this theory to the dissolution of flufenamic acid in tablets is described.

Keywords——dissolution kinetics; available surface area; Weibull distribution; log-normal distribution; solid dosage form; linear regression; non-linear regression; numerical calculation; flufenamic acid

For the prediction of bioavailability of solid dosage forms, the dissolution test is commonly used as an *in vitro* evaluation test due to the simplicity of the method. However, the information that can be gained from the dissolution test is the total amount of dissolved drug, which is influenced by numerous factors (solubility, available surface area, diffusion coefficient, disintegration time, *etc.*).

The theoretical consideration of dissolution kinetics has been attempted through two approaches. One approach has been developed by extending the dissolution theory of monodisperse powders as represented by the Hixson–Crowell cube root equation[2)] to the dissolution kinetics of polydisperse powders. This approach was first presented by Higuchi and Hiestand.[3,4)] Recently Brooke,[5,6)] and Pedersen[7)] derived an exact dissolution rate equation in relation to the log-normal distribution. In addition, Kitamori *et al.*[8)] applied the theory to nonspherical powders. However, this approach relies on the assumption of a sink condition and its application is restricted almost entirely to powders, not to pharmaceutical preparations.

Another approach is based on the curve fitting of the dissolution patterns by using the probability distribution.[9,10)] In this approach, though the theoretical data coincide with most of the experimental data, the complex mechanism of the dissolution process cannot be elucidated.

In the present study, time course equations of $S(t)$ generated in the dissolution process were derived and the influence of the manufacturing process on the dissolution of flufenamic acid in tablets was evaluated in terms of the time course of $S(t)$.

Theoretical

The Time Course Equations for Available Surface Area

The dissolution rate from an organic solid surface is generally considered to be diffusion-controlled, given by the Noyes–Whitney equation[11] as follows:

$$dC/dt = k \cdot S/V \cdot (Cs - C) \tag{1}$$

where k is the rate constant per unit area, S is the available surface area, V is the solvent volume, Cs is the solubility, and C is the solute concentration.

When the available surface area is not constant, Eq. 1 can be rewritten as

$$dC/dt = k \cdot S(t)/V \cdot (Cs - C) \tag{2}$$

After integration and rearrangement of Eq. 2, we have

$$\int_0^t S(t)dt = V/k \cdot \ln(Cs/(Cs - C)) \tag{3}$$

As the surface of the drug is renewed at every stage of the dissolution process, the integral value of $S(t)$ is interpreted as the total available surface area generated from the initial time to time t. Similarly, the total available surface area generated during the dissolution process is given by

$$\int_0^\infty S(t)dt = V/k \cdot \ln(Cs/(Cs - Wo/V)) \tag{4}$$

where Wo is the initial amount of the drug in solid dosage forms ($Wo < Cs \cdot V$).

When Eq. 3 is divided by Eq. 4, the following equation is obtained.

$$F(t) = \int_0^t S(t)dt \Big/ \int_0^\infty S(t)dt = \ln(Cs/(Cs - C))/\ln(Cs/(Cs - Wo/V)) \tag{5}$$

where $F(t)$ is interpreted as the ratio of the cumulative surface area which has been made available for dissolution up to time t to the total surface area which is made available during the dissolution process,[9] and $F(t)$ at any time can be calculated from the experimental data (Cs, C). Differentiating Eq. 5 with respect to t produces

$$S(t) = V/k \cdot \ln(Cs/(Cs - Wo/V)) \cdot dF(t)/dt \tag{6}$$

From rearrangement of Eq. 5, the theoretical dissolution rate equation in relation to $S(t)$ is obtained as

$$C = Cs(1 - \exp(-(\ln(Cs/(Cs - Wo/V)) \cdot F(t)))) \tag{7}$$

In addition, since $F(t)$ has the following character:

$$\text{when } t = 0 \qquad F(0) = \int_0^0 S(t)dt \Big/ \int_0^\infty S(t)dt = 0 \tag{8}$$

$$\text{when } t = \infty \qquad F(\infty) = \int_0^\infty S(t)dt \Big/ \int_0^\infty S(t)dt = 1 \tag{9}$$

it can be interpreted as a cumulative probability distribution. Thus, $F(t)$ can be rewritten as

$$F(t) = \int_0^t \phi(t)dt \tag{10}$$

where $\phi(t)$ is the probability distribution. Substituting Eq. 10 into Eqs. 6 and 7 gives

$$S(t)=V/k\cdot\ln(Cs/(Cs-Wo/V))\cdot\phi(t) \tag{11}$$

$$C=Cs(1-\exp(-(\ln(Cs/(Cs-Wo/V))\cdot\int_0^t\phi(t)\mathrm{d}t))) \tag{12}$$

On the basis of this theory, $S(t)$ in the dissolution process and the theoretical dissolution rate in relation to $S(t)$ of a solid dosage form can be determined as follows:

(1) Measurement of Cs and k.
(2) Determination of $F(t)$ at appropriate times of the dissolution test by using Eq. 5.
(3) Finding the best-fitting parameters for the probability distribution of the values of $F(t)$ by using linear regression or non-linear regression.
(4) Substitution of experimental data (Cs, k, Wo, V) and the values of the probability distribution parameters into Eqs. 11 and 12.

Selection of Probability Distributions

In this report, the Weibull distribution and log-normal distribution were adopted as $\phi(t)$ because they cover extensive distribution patterns. The Weibull distribution is shown in Eq. 13

$$\phi(t)=b/a\cdot t^{b-1}\exp(-(t^b/a)) \tag{13}$$

where a is the scale parameter and b is the shape parameter. By substituting Eq. 13 into Eqs. 10—12, $F(t)$, $S(t)$ and C can be calculated as follows.

$$F(t)=1-\exp(-(t^b/a)) \tag{14}$$

$$S(t)=b\cdot V/(a\cdot k)t^{b-1}\cdot\ln(Cs/(Cs-Wo/V))\cdot\exp(-(t^b/a)) \tag{15}$$

$$C=Cs(1-\exp(-(\ln(Cs/(Cs-Wo/V))\cdot(1-\exp(-(t^b/a)))))) \tag{16}$$

Similarly, if the log-normal distribution is adopted, $\phi(t)$ can be written as

$$\phi(t)=1/(\sqrt{2\pi}\cdot\sigma\cdot t)\exp(-((\ln t-\ln\mu)^2/(2\cdot\sigma^2))) \tag{17}$$

where μ is the logarithmic mean of t and σ is the standard deviation. Then $F(t)$ $S(t)$ and C are given by

$$F(t)=1/(\sqrt{2\pi}\cdot\sigma)\cdot\int_0^{\ln t}\exp(-(\ln t-\ln\mu)^2/(2\cdot\sigma^2))\mathrm{d}(\ln t) \tag{18}$$

$$S(t)=V/(\sqrt{2\pi}\cdot\sigma\cdot k\cdot t)\cdot\ln(Cs/(Cs-Wo/V))\cdot\exp(-(\ln t-\ln\mu)^2/(2\cdot\sigma^2)) \tag{19}$$

$$C=Cs(1-\exp(-(1/(\sqrt{2\pi}\cdot\sigma)\cdot\ln(Cs/(Cs-Wo/V))\times\int_0^{\ln t}\exp(-(\ln t-\ln\mu)^2/(2\cdot\sigma^2))\mathrm{d}(\ln t)))) \tag{20}$$

Experimental

Materials——Flufenamic acid (FFA) was of commercial grade. Carboxymethyl cellulose calcium (CMC-Ca), hydroxypropyl cellulose (HPC-L), microcristalline cellulose (MCC) and magnesium stearate (St. Mg) were all of JP X grade. All other chemicals were of reagent grade.

Preparations of FFA (100 mg) Tablets——The manufacturing process and formulas for the samples are shown in Table I and their properties are listed in Table II. The formulas of all the tablets were almost the same except for the amount of binder (HPC-L), but each tablets was made by using a different granulating process. Rp. 1 was prepared by granulating FFA, Rp. 2 was prepared by granulating a mixture of FFA and CMC-Ca and Rp. 3 was prepared by granulating a mixture of FFA, MCC and CMC-Ca.

Dissolution Study——Dissolution of FFA from the preparations was tested in a USP dissolution test apparatus (Method II) in a pH 6.2 phosphate buffer agaitated at 100 rpm, at 37 °C. A 2 ml aliquot of sample solution was

TABLE I. The Manufacturing Process and Formulas for the FFA (100 mg) Tablets

Lot. No.	Ingredient (mg/t)	Manufacturing process
Rp. 1	FFA 100 HPC-L[a] 4 MCC 158 CMC-Ca 30 St. Mg 5	kneading—drying—granulating mixing—tableting (10 mmϕ) (297 mg/t)
Rp. 2	FFA 100 CMC-Ca 30 HPC-L 6 MCC 156 St. Mg 5	mixing—kneading—drying—granulating mixing—tableting (10 mmϕ) (297 mg/t)
Rp. 3	FFA 100 MCC 150 CMC-Ca 30 HPC-L 12 St. Mg 5	mixing—kneading—drying—granulating mixing—tableting (10 mmϕ) (297 mg/t)

a) Used as aqueous solution.

TABLE II. The Properties of FFA (100 mg) Tablets

Lot. No.	Disintegration time (min)	Hardness (kg)	Thickness (mm)
Rp. 1	2—4	4.4	4.0
Rp. 2	2—4	5.4	3.9
Rp. 3	2—4	4.5	3.9

withdrawn at appropriate intervals through a membrane filter (pore diameter: 0.45 μ) and immediately replaced with 20 ml of the phosphate buffer. The absorpbance was determined at 288 nm with a spectrophotometer and the FFA concentration was calculated from the absorbance of the standard solution.

Rotating Disk Method——In order to determine k, the rotating disk method was used. An FFA disk having a diameter of 2 cm was prepared by compressing 500 mg of the drug powder at a pressure of 500 kg/3.14 cm^2. The disk was stuck perpendicularly to a rotating shaft with an adhesive so that only one of the planar surfaces was exposed (S=3.14 cm^2). The shaft was set in a USP dissolution test apparatus, and rotated at 100 rpm in a pH 6.2 phosphate buffer at 37 °C. A 5 ml aliquot of the solution was withdrawn at appropriate intervals and after adequate dilution, the FFA concentration was calculated spectrophotometrically by the same method as was applied in the dissolution study.

Determination of Apparent Solubility, *Cs*——FFA (1 g) was added to a pH 6.2 phosphate buffer (200 ml) at 37 °C, and the mixture was agitated at 800 rpm for 3 h. The apparent solubility (Cs) of FFA was obtained in the same manner as described in the dissolution study.

Results and Discussion

Computer Simulations of $S(t)$ and C *vs.* t Patterns

The influence of probability parameters on the time course of $S(t)$ and C was simulated on a microcomputer. The patterns in relation to the Weibull distribution are shown in Figs. 1—4. When the shape parameter was constant ($b=2$), the $S(t)$ *vs.* t pattern calculated from Eq. 15 was sharper and the peak time eventually approached the initial time as the scale parameter (a) decreased (Fig. 1), whreas the dissolution rate (C) calculated from Eq. 16 increased (Fig. 2). Since the differential value of Eq. 13 becomes zero at the peak time ($=t_{max}$).

$$b/at_{max}^{b-2}\cdot((b-1)-b/at_{max}^{b})\cdot\exp(-(t_{max}^{b}/a))=0 \tag{21}$$

Then

$$t_{max}=\sqrt[b]{a(b-1)/b} \tag{22}$$

Furthermore, when $Td=\sqrt[b]{a}$ was substituted into Eq. 14,

$$F(Td)=1-\exp(-1)\fallingdotseq 0.632 \tag{23}$$

Thus, Td is considered to be the time when the 63.2% of the available surface area ($S(t)$) has been generated during the dissolution process. The values of t_{max} and Td in Fig. 1 are shown in Table III.

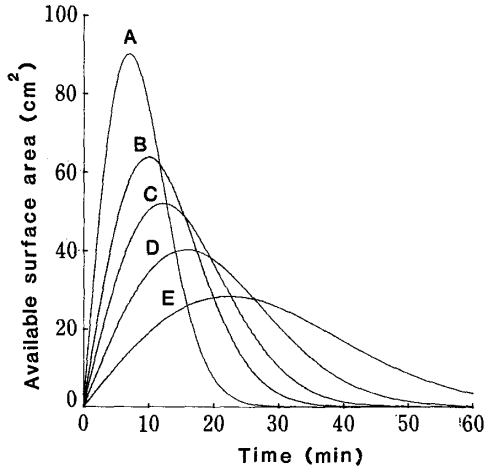

Fig. 1. The Influence of Parameter a of the Weibull Distribution on the $S(t)$ *vs.* t Patterns ($b=2$)

$Cs=1000$ mg/l; $k=0.1$ cm/min; $Wo=100$ mg; $V=1$ l. A, $a=100$; B, $a=200$; C, $a=300$; D, $a=500$; E, $a=1000$.

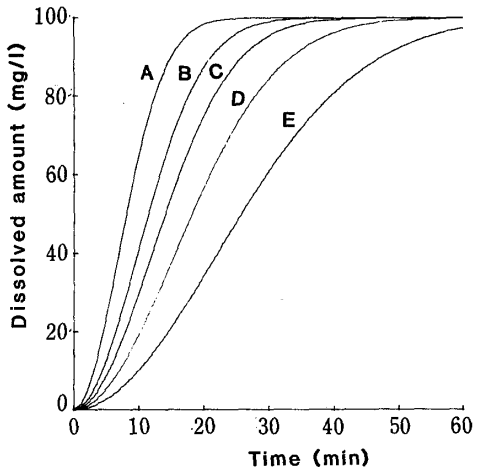

Fig. 2. The Influence of Parameter a of the Weibull Distribution on the Dissolution Rate in Relation to $S(t)$ ($b=2$)

The symbols are the same as in Fig. 1.

TABLE III. The Probability Parameters of the Weibull Distribution in Fig. 1

Symbol	Probability parameters			
	a	b	t_{max} (min)	Td (min)
A	100	2	7.07	10.0
B	200	2	10.0	14.1
C	300	2	12.2	17.3
D	500	2	15.8	22.4
E	1000	2	22.4	31.6

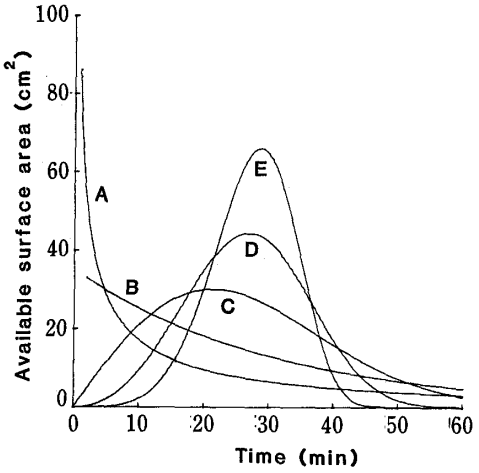

Fig. 3. The Influence of Parameter b of the Weibull Distribution on the $S(t)$ *vs.* t Patterns ($Td=30$ min)

$Cs=1000$ mg/l; $k=0.1$ cm/min; $Wo=100$ mg; $V=1$ l. A, $b=0.5$; B, $b=1$; C, $b=2$; D, $b=3.26$; E, $b=5$.

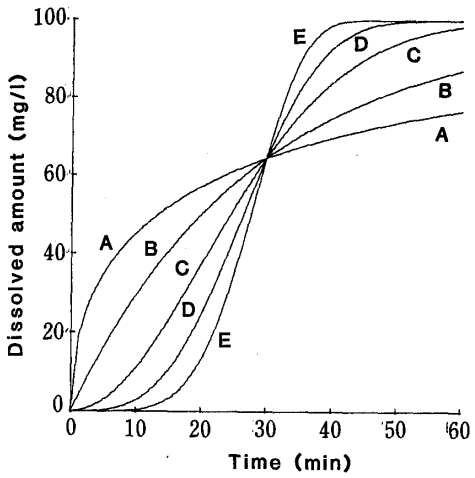

Fig. 4. The Influence of Parameter b of the Weibull Distribution on the Dissolution Rate in Relation to $S(t)$ ($Td=30$ min)

The symbols are the same as in Fig. 3.

TABLE IV. The Probability Parameters of the Weibull Distribution in Fig. 3

Symbol	Probability parameters			
	a	b	t_{max} (min)	Td (min)
A	5.48	0.5	—	30
B	30	1	—	30
C	9.00×10^{2}	2	21.2	30
D	6.54×10^{4}	3.26	26.8	30
E	2.43×10^{7}	5	28.8	30

Figure 3 shows the influence of the shape parameter (b) on the time course of $S(t)$ under the condition of $Td=30$ min. When $b\leqq1$, the $S(t)$ *vs.* t pattern had a downward curvature, whereas when $b>1$, it had a maximum which was sharper and the time of which was more remote from the initial time as the shape parameter (b) increased. Figure 4 shows the dissolution patterns calculated from Eq. 16. As the shape parameter (b) increased, the C *vs.* t pattern showed a sigmoid curve and the dissolution rate increased. Furthermore, each pattern coincided at Td ($=30$ min). The values of t_{max} and a are shown in Table IV.

In general, $S(t)$ of tablets is initially increased due to disintegration and deaggregation and subsequently decreased due to dissolution. Thus, the $S(t)$ *vs.* t patterns of tablets may be analyzed under the condition of $b>1$. On the other hand, $S(t)$ of granules and capsules is always decreased due to dissolution. Thus, these $S(t)$ *vs.* t patterns may be analyzed under the condition of $b\leqq1$.

The patterns in relation to log-normal distribution are shown in Figs. 5—8. When the logarithmic mean was constant ($\mu=20$ min), the $S(t)$ *vs.* t pattern calculated from Eq. 19 was sharper and the peak time (t_{max}) was more remote from the initial time, as the standard deviation increased (Fig. 5), whereas the dissolution rate (C) calculated from Eq. 20 became sigmoid and each pattern coincided at the point of $t=20$ min (Fig. 6), where the integral of Eq. 20 was determined by using the Hastings approximate equations:

$$Z=(\ln t-\ln\mu)/\sigma \tag{24}$$

$$P(Z)=1/\sqrt{2\pi}\cdot\int_{-\infty}^{Z}\exp(-Z^2/2)\mathrm{d}Z=\begin{cases}G(X) & Z\geqq 0\\ 1-G(Z) & Z<0\end{cases} \tag{25}$$

$$X=1/(1+0.2316419\cdot Z) \tag{26}$$

$$G(Z)=1/\sqrt{2\pi}\cdot\exp(-Z^2/2)\cdot(C_1\cdot X+C_2\cdot X^2+C_3\cdot X^3+C_4\cdot X^4+C_5\cdot X^5) \tag{27}$$

$C_1=$ 0.319381530 $C_2=-0.356563782$ $C_3=1.78147937$

$C_4=-0.1821255978$ $C_5=$ 1.330274429

On the other hand, since the differential value of Eq. 17 becomes zero at the point of the peak time (t_{max}),

$$1/(\sqrt{2\pi}\cdot\sigma\cdot t)\cdot(1+(\ln t_{max}-\ln\mu)/\sigma^2)\exp(-(\ln t_{max}-\ln\mu)^2/(2\cdot\sigma^2))=0 \tag{28}$$

then

$$t_{max}=\exp(\ln\mu-\sigma^2) \tag{29}$$

The values of t_{max} in Fig. 5 are shown in Table V. When the standard deviation was constant ($\sigma=0.4$), the $S(t)$ *vs.* t pattern calculated from Eq. 19 was sharper and the peak time (t_{max}) eventually approached the initial time as the logarithmic mean (μ) decreased (Fig. 7), whereas the dissolution rate increased (Fig. 8). The values of t_{max} in Fig. 7 are shown in Table VI.

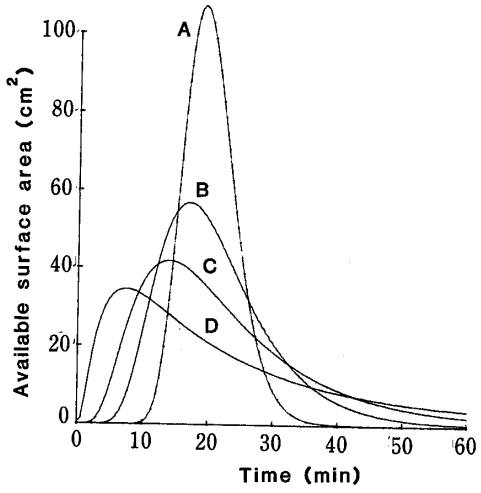

Fig. 5. The Influence of Parameter σ of log-Normal Distribution on the $S(t)$ *vs.* t Patterns ($\mu=20$ min)

$Cs=1000$ mg/l; $k=0.1$ cm/min; $Wo=100$ mg; $V=1$ l. A, $\sigma=0.2$; B, $\sigma=0.4$; C, $\sigma=0.6$; D, $\sigma=1.0$.

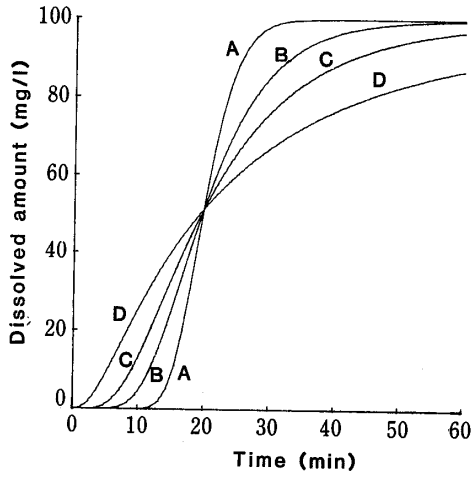

Fig. 6. The Influence of Parameter σ of log-Normal Distribution on the Dissolution Rate in Relation to $S(t)$ ($\mu=20$ min)

The symbols are the same as in Fig. 5.

TABLE V. The Probability Parameters of the log-Normal Distributions in Fig. 5

Symbol	Probability parameters		
	σ	μ (min)	t_{max} (min)
A	0.2	20	19.2
B	0.4	20	17.0
C	0.6	20	14.0
D	1.0	20	7.4

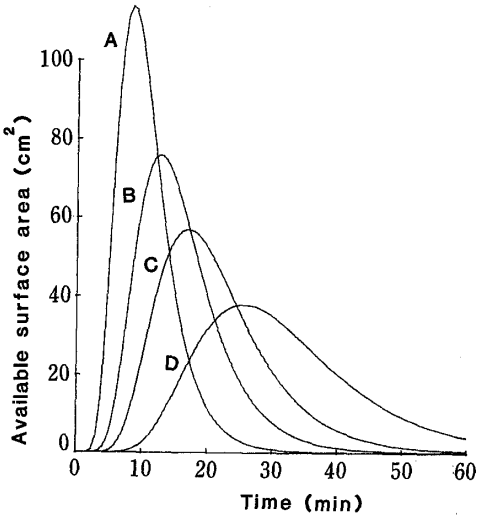

Fig. 7. The Influence of Parameter μ of log-Normal Distribution on the $S(t)$ *vs.* t Patterns ($\sigma=0.4$)

$Cs=1000$ mg/l; $k=0.1$ cm/min; $Wo=100$ mg; $V=1$ l. A, $\mu=10$ min; B, $\mu=15$ min; C, $\mu=20$ min; D, $\mu=30$ min.

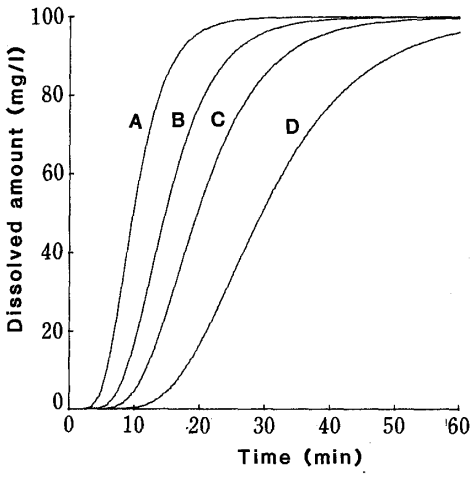

Fig. 8. The Influence of Parameter μ of log-Normal Distribution on the Dissolution Rate in Relation to $S(t)$ ($\sigma=0.4$)

The symbols are the same as in Fig. 7.

TABLE VI. The Probability Parameters of the log-Normal Distributions in Fig. 7

Symbol	Probability parameters		
	σ	μ (min)	t_{max} (min)
A	0.4	10	8.5
B	0.4	15	12.8
C	0.4	20	17.0
D	0.4	30	25.6

Determination of *k*

The results of the dissolution test on an FFA disk using the rotating disk method are shown in Fig. 9. An approximately linear relationship existed between time and the dissolved amount of FFA. If $Cs \gg C$ (sink condition) and $S=$constant, then from the rearrangement and integration of Eq. 1

$$C=k\cdot S\cdot Cs/V\cdot t \tag{30}$$

Linear regression of the experimental data produces Eq. 31.

$$C=0.126\cdot t+0.166 \qquad r=0.997 \tag{31}$$

From the slope of Eqs. 30 and 31, $k=9.63\times10^{-2}$ cm/min was obtained.

***S(t) vs. t* Patterns of the FFA (100 mg) Tablets**

$F(t)$ of the Weibull distribution shown in Eq. 14 may be rearranged into

$$\ln\cdot\ln(1/(1-F(t)))=b\cdot\ln t-\ln a \tag{32}$$

Based on Eq. 32, linear plots for FFA (100 mg) tablets were obtained in the ln ln–ln plot (Weibull plot) of $1/(1-F(t))$ *vs.* t (see Fig. 10). On the other hand, by substituting Eqs. 18 and 24 with Eq. 25, $F(t)$ of the log-normal distribution could be rewritten as

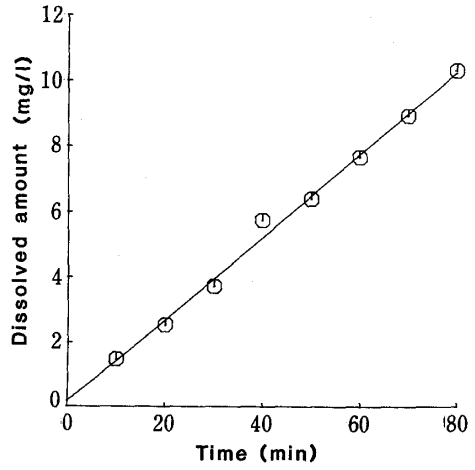

Fig. 9. Dissolution Rate of an FFA Disk by the Rotating Disk Method

$S=3.14\,cm^2$; $Cs=375$ mg/l; $V=900$ ml. The ① are experimental data and the full line is the regression line.

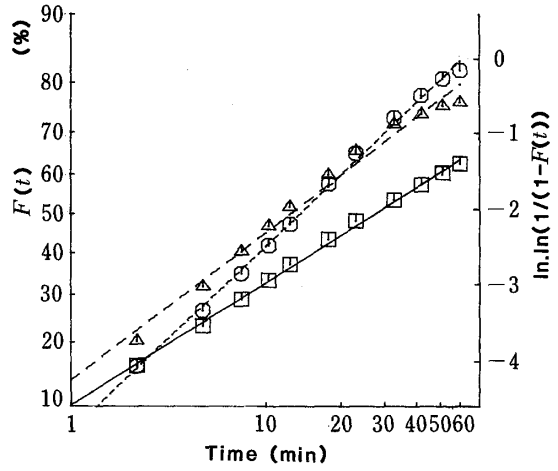

Fig. 10. Weibull Plot for $F(t)$ of FFA (100 mg) Tablets

Lot. No.	Experimental data	Regression line
Rp. 1	①	——
Rp. 2	△	- - - -
Rp. 3	①	------

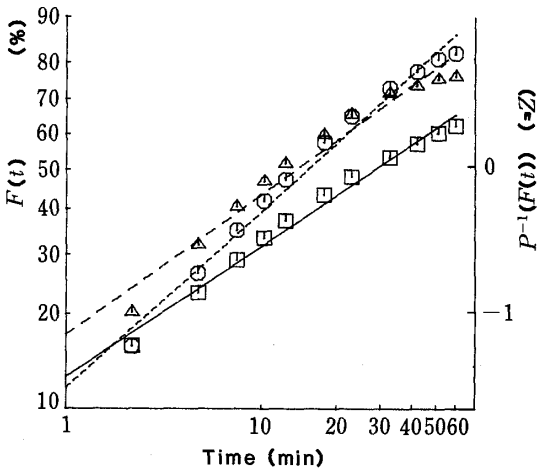

Fig. 11. log-Normal Plot for $F(t)$ of FFA (100 mg) Tablets

Lot. No.	Experimental data	Regression line
Rp. 1	①	——
Rp. 2	△	- - - -
Rp. 3	①	------

$$F(t)=1/\sqrt{2\pi}\cdot\int_{-\infty}^{z}\exp(-Z^2/2)\mathrm{d}Z=P(Z) \tag{33}$$

Then, Eq. 33 could be rearranged as

$$Z=P^{-1}(F(t))=(\ln t-\ln\mu)/\sigma \tag{34}$$

where the $P^{-1}(Z)$ is the inverse function of $P(Z)$. The solution of $P^{-1}(Z)$ was determined by using the Hastings approximate equations:

$$Q=1-F(t) \tag{35}$$

$$X=\sqrt{\ln(1/Q^2)} \tag{36}$$

$$Z=P^{-1}(F(t))=X-(C_0+C_1\cdot X+C_2\cdot X^2)/(1+d_1\cdot X+d_2\cdot X^2+d_3\cdot X^3) \tag{37}$$

$C_0=2.515517$ $C_1=0.802853$ $C_2=0.010328$

$d_1=1.432788$ $d_2=0.189269$ $d_3=0.00138$

From Eqs. 35—37, linear relationships of $F(t)$ of the FFA (100 mg) tablets were obtained for

TABLE VII. The Probability Parameters of $S(t)$ of FFA (100 mg) Tablets

Lot. No.	Weibull distribution					log-Normal distribution			
	a	b	t_{max} (min)	Td (min)	r (AIC)[c]	σ	μ (min)	t_{max} (min)	r (AIC)
Rp. 1	7.38[a]	0.505	—	52.4	0.994	2.58	24.4	3.14×10^{-2}	0.999
	(6.77)[b]	(0.477)		(55.1)	(−61.0)	(2.58)	(24.4)	(3.14×10^{-2})	(−77.3)
Rp. 2	5.30	0.540	—	21.9	0.982	2.14	10.0	1.02×10^{-1}	0.992
	(4.82)	(0.513)		(21.5)	(−45.3)	(2.11)	(9.87)	(1.15×10^{-1})	(−55.3)
Rp. 3	8.05	0.679	—	21.6	0.993	1.72	11.1	5.76×10^{-1}	0.999
	(7.32)	(0.654)		(21.0)	(−52.6)	(1.69)	(11.1)	(6.38×10^{-1})	(−73.6)

a) The values determined by linear regression. *b*) The values determined by non-linear regression. *c*) $AIC=N\cdot\ln(Re)+2P$: N=number of experimental data points; Re=residual sum of squares; P=number of parameters in estimated model.

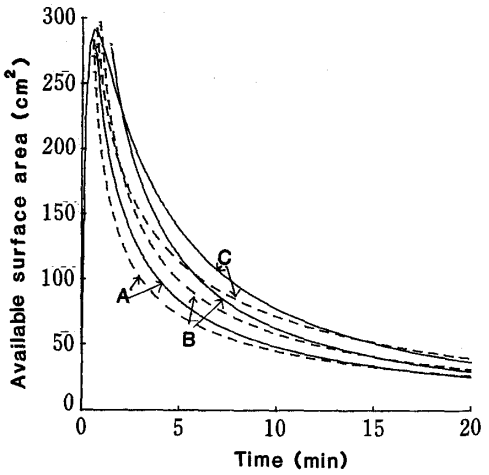

Fig. 12. The $S(t)$ *vs.* t Patterns of FFA (100 mg) Tablets

Cs=375 mg/l; Wo=100 mg; V=900 ml; $k=9.63\times10^{-2}$ cm/min. The broken lines are regression curves of the Weibull distribution, and the full lines are regression curves of the log-normal distribution. Each probability parameter was determined by non-linear regression.
A, Rp. 1; B, Rp. 2; C, Rp. 3.

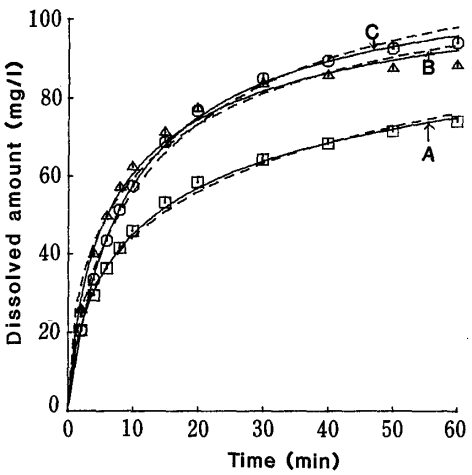

Fig. 13. The Dissolution Rate of FFA (100 mg) Tablets

Cs=375 mg/l; Wo=100 mg; V=900 ml. The broken lines are regression curves of the Weibull distribution and the full lines are the regression curves of the log-normal distribution. Each probability parameter was determined by non-linear regression.

Lot. No.	Experimental data	Regression line
Rp. 1	□	A
Rp. 2	△	B
Rp. 3	○	C

the P^{-1} ($F(t)$)−ln plot (log-normal plot) of $F(t)$ *vs.* t (see Fig. 11). By means of linear regression of the data in Figs. 10 and 11, the approximate values of the probability parameters for the FFA (100 mg) tablets were obtained from Eqs. 38—41,

$$a=\exp(-Yo) \tag{38}$$

$$b=A \tag{39}$$

$$\sigma=1/A \tag{40}$$

$$\mu=\exp(-A/Yo) \tag{41}$$

where A is the slope and Yo is the y-intercept of the line. Furthermore, the best-fit values of the probability parameters were determined by non-linear regression (simplex method)[12] using the approximate values obtained from Eqs. 38—41 as the initial values. The probability

parameters of the FFA (100 mg) tablets are shown in Table VII. The fit of the experimental data was estimated in terms of the correlation coefficient (r) and Akaike's information criterion (AIC).[13] There was little difference between the values obtained by using linear regression and non-linear regression, but the log-normal distribution was a little more suitable for the curve fitting of $F(t)$ for the FFA (100 mg) tablets.

By substituting the determined values of the probability distributions, Wo, V, k and Cs into Eqs. 15, 16, 19 and 20, the time course of $S(t)$ and the dissolution rate in relation to $S(t)$ of the FFA (100 mg) tablets were obtained. The results are shown in Figs. 12 and 13.

In this experiment, a well-defined t_{max} could not be obtained due to the fact that the initial dissolution rates of the FFA (100 mg) tablets were too fast to obtain the sigmoid curve of the dissolution patterns. However, since the experimental data coincided with the regression curves in Fig. 13, the $S(t)$ values in Fig. 12 were assumed to be reasonable. Though each lot of the FFA (100 mg) tablets had the same disintegration time in Table II, the tablet which was prepared by granulating FFA (Rp. 1) gave the smallest dissolution rate and value of $S(t)$ generated, whereas the tablet which was prepared by granulating the mixture of FFA, MCC and CMC-Ca (Rp. 3) gave the largest dissolution rate and value of $S(t)$ generated. Since the value of $S(t)$ generated was in good agreement with the dissolution rate, the difference of the dissolution patterns in Fig. 13 is thought to be responsible for the difference of available surface area generated during the deaggregation process of disintegrated granules.

References and Notes

1) This paper forms Part I of "Dissolution Profile in Relation to Available Surface Area." This work was presented at the 101st Annual Meeting of the Pharmaceutical Society of Japan, Kumamoto, April 1981.
2) A. Hixson and Crowell, *J. Ind. Eng. Chem.*, **23**, 923 (1931).
3) W. I. Higuchi and E. N. Hiestand, *J. Pharm. Sci.*, **52**, 67 (1963).
4) W. I. Higuchi, E. L. Rove and E. N. Hiestand, *J. Pharm. Sci.*, **52**, 162 (1963).
5) D. Brooke, *J. Pharm. Sci.*, **62**, 795 (1973).
6) D. Brooke, *J. Pharm. Sci.*, **63**, 344 (1974).
7) P. V. Petersen and K. F. Brown, *J. Pharm. Sci.*, **64**, 1193 (1975).
8) N. Kitamori and K. Iga, *J. Pharm. Sci.*, **67**, 1674 (1978).
9) J. G. Wagner, *J. Pharm. Sci.*, **58**, 1253 (1969).
10) F. Langenbucher, *J. Pharm. Pharmacol.*, **24**, 979 (1972).
11) A. W. Noyes and W. Whitney, *J. Am. Chem. Sci.*, **19**, 930 (1897).
12) Non-linear regressions were performed using the MULTI program devised by K. Yamaoka and U. Tanikawara.
13) K. Yamaoka, T. Nakagawa and T. Uno, *J. Pharmacokin. Biopharm.*, **6**, 165 (1978).